Department of Plastic and Cosmetic Surgery[1], The Second Affiliated Hospital of Soochow University, Suzhou; Clinical College of Integrated Traditional Chinese and Western Medicine[2]; Department of Neurology[3], The First Affiliated Hospital, Anhui University of Traditional Chinese Medicine, Hefei, China

Anti-inflammatory effects of ginsenoside Rg3 on the hypertrophic scar formation via the NF-κB/IκB signaling pathway in rabbit ears

L. Ma[1,2,#], L.Y. Li[3,#] T.L. Zhao[1,*]

Received October 27, 2019, accepted November 22, 2019

**Corresponding author: Tian-Lan Zhao, MD, PhD, Department of Plastic and Cosmetic Surgery, The Second Affiliated Hospital of Soochow University, 1055 Sanxiang Road, Suzhou, Jiangsu, 215004, China*
ztlsdefy@163.com
[#]Li Ma and Liang-Yong Li contributed equally to this work.

Pharmazie 75: 102-106 (2020) *doi: 10.1691/ph.2020.9852*

The anti-inflammatory effects of Rg3 on the hypertrophic scar (HS) formation remain relatively obscure. Hence, this study aimed to explore the anti-inflammatory effects of Rg3 on the HS formation using a rabbit ear model and we assessed the involvement of the NF-κB/IκB signaling pathway in this process. We constructed the Newland white rabbit ear HS model and treated it with Rg3. Using histological analyses, we evaluated scar hypertrophy based on the hematoxylin and eosin staining. The degree of scarring was evaluated using the scar elevation index (SEI). In addition, collagen I and collagen III expression levels were assessed by immunohistochemistry, while fibroblast apoptosis was examined using TUNEL assays. While MPO, IL-1β, IL-6, and TNF-α concentrations were quantified using ELISA, NF-κB and p-IκB activities were respectively measured using electrophoretic mobility shift assays (EMSAs) and western blots. SEI measurements and histological characteristics revealed that Rg3 could suppress the HS formation. Moreover, Rg3 could inhibit the HS formation by decreasing collagen I and collagen III synthesis and inducing fibroblast apoptosis. Besides, Rg3 treatment markedly inhibited the inflammatory cytokine production and ameliorated neutrophil infiltration. Notably, this study revealed that Rg3 inhibited NF-κB activation and the activity of p-IκB. Furthermore, this study suggested that the ability of Rg3 to decrease the scar formation might result from its ability to inhibit inflammation by modulating the NF-κB/IκB signaling. Overall, the findings of this study could support the use of Rg3 to prevent the HS formation.

1. Introduction

Hypertrophic scar (HS), a common and inevitable consequence of tissue repair and wound healing, is characterized by the proliferation of fibroblasts and excessive accumulation of collagen (Sorg et al. 2017; Lee and Jang 2018). Individuals with HS experience significant aesthetic and functional disorders, along with negative psychological effects, including pain, stiffness, pruritus decreased self-esteem, mental distress, and even functional impairment when it affects joints. Clinical efforts to relieve patient pain have employed a wide range of approaches including the application of pressure, intralesional steroids, surgical excision, cryotherapy, or laser-based therapy. However, these treatments are associated with poor efficacy, high rates of recurrence, or the potential for significant and undesirable side effects, thereby negatively affecting patients' satisfaction (Lee and Jang 2018). Thus, a valid therapeutic approach for the treatment of HS is urgently needed.

Skin wound healing is a complex biological process that encompasses the following three overlapping phases: inflammation, proliferation, and remodeling. During the initial wound inflammation phase, inflammatory cells are recruited and activated, with a marked secretion of cytokines at the wound site that, in turn, affect subsequent wound healing. Proper healing of tissue injuries is dependent both upon the initiation and appropriate termination of a proportional inflammatory response. When such inflammation becomes dysregulated, this can markedly impair normal tissue repair. Such excessive inflammation has recently been shown to be closely associated with HS formation, with the production of inflammatory cytokines such as interleukin 6 (IL-6), IL-1β, tumor necrosis factor-α (TNF-α), and transforming growth factor (TGF)-β1, produced by inflammatory cells stimulating fibroblast proliferation and excessive collagen accumulation (Qian et al. 2016; Sorg et al. 2017). In addition, early anti-inflammatory treatment at a wound site could efficiently prevent HS formation (Liu et al. 2014; Wang et al. 2015; Shan et al. 2017). A growing body of evidence has suggested that the nuclear factor kappa B (NF-κB)/IκB signaling pathway is essential for the regulation of inflammation (Rothschild et al. 2018; Staal and Beyaert 2018). Reportedly, the NF-κB/IκB signaling participates in the HS formation. Gong et al. (2017) reported that the expressions of NF-κB mRNA and protein increased in HS fibroblasts. Chen et al. demonstrated that expressions of NF-κB and p-IκBa upregulated in HS in rabbit ears but downregulated NF-κB and p-IκBa could contribute to papain elastic liposomes against the HS formation (Ishise et al. 2015; Chen et al. 2017; Gong et al. 2017). Thus, targeting the NF-κB pathway could offer a novel method for the treatment of HS. However, limited information is available about the role of NF-κB/IκB signaling pathway-mediated inflammation in the HS formation.

As a traditional Chinese medicine isolated from *Panax ginseng*, ginsenoside Rg3 (Rg3) contains a wide array of pharmacological characteristics, including anti-inflammatory and antitumor properties (Wang et al. 2015; Lee et al. 2016). In addition, ginsenoside Rg3 reportedly suppresses the NF-κB/IκB signaling pathway in the treatment of asthma and acute lung injury in mice (Cheng and Li 2016; Lee et al. 2016). A recent study reported that Rg3 could alleviate HS formation by inhibiting fibroblast proliferation, downregulating VEGF expression, and suppressing early exacerbated inflammation without adverse effects in a rabbit ear model (Cheng et al. 2014). However, as the assessment

of anti-inflammatory effects of Rg3 against the HS formation has only been done using the hematoxylin and eosin (H&E) staining of histological observation, the detailed underlying molecular mechanisms involved remain unclear. Hence, we hypothesized that ginsenoside Rg3 could also possess anti-inflammatory effects in the context of the HS formation by targeting the NF-κB/IκB signaling pathway.

This study aimed to investigate the anti-inflammatory efficacy of Rg3 in a rabbit ear model of the HS formation, examining inflammatory cell infiltration, inflammatory cytokine release, and evaluating the NF-κB/IκB signaling pathway activation.

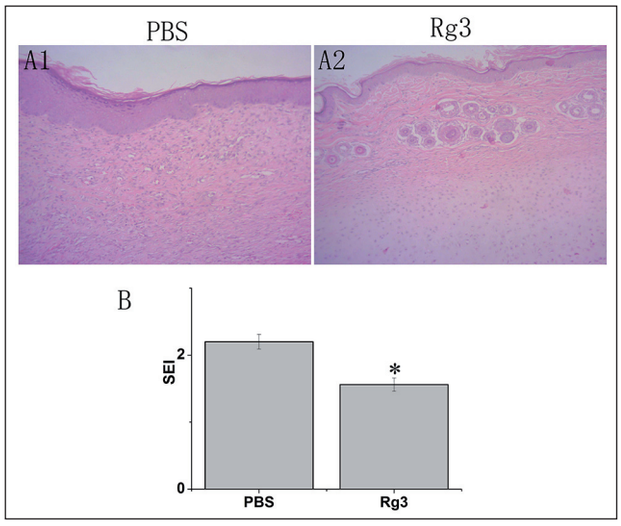

Fig. 1: Hematoxylin and eosin (H&E) histological staining. (A1 and A2) Scarring in the PBS-treated and Rg3-treated groups, respectively. The epidermal and dermal layers in the PBS-treated scars were obviously thickened, with abundant fibroblasts and rich microvessels. Conversely, the Rg3-treated group exhibited less thick, more regular, and fewer proliferative cells and capillaries. Scale bar, 20 μm. (B) The average scar elevation index (SEI) values, with values for Rg3-treated samples being lower than PBS-treated controls (*$P < 0.05$, $n = 18$).

2. Investigations and results

2.1. Histological characteristics and scar elevation index (SEI)

We performed H&E staining to investigate the anti-scarring properties of Rg3 on rabbit ear wounds. The epidermal and dermal layers in the PBS-treated scars were clearly thickened (Fig. 1). In addition, collagen fibers were disorganized and dense, and we observed abundant fibroblasts with rich microvessels. Conversely, the Rg3-treated group exhibited a less thick, more regular, and loose collagen distribution with fewer proliferative cells and capillaries.

The mean SEI of the PBS-treated groups was 2.20±0.11, whereas that in the Rg3-treated group was significantly lower at 1.56 ± 0.10 ($P < 0.05$; Fig. 1).

2.2. Impact of Rg3 on the HS cell apoptosis

We assessed the levels of apoptotic cell death, based on the frequency of TUNEL-positive cells, which were significantly increased upon Rg3 treatment compared with PBS controls ($P < 0.05$), illustrating that Rg3 could induce the HS cell apoptosis (Fig. 2).

2.3. Impact of Rg3 on collagen synthesis

To determine whether Rg3 affected the levels type I and III collagen, which are crucial for extracellular matrix (ECM) composition, we conducted immunohistochemical staining of the scar area. The Rg3-treated group exhibited significantly lower levels of type I and III collagen compared with PBS controls ($P < 0.05$; Fig. 3), thereby suggesting that Rg3 could suppress collagen synthesis (Fig. 3 and 4).

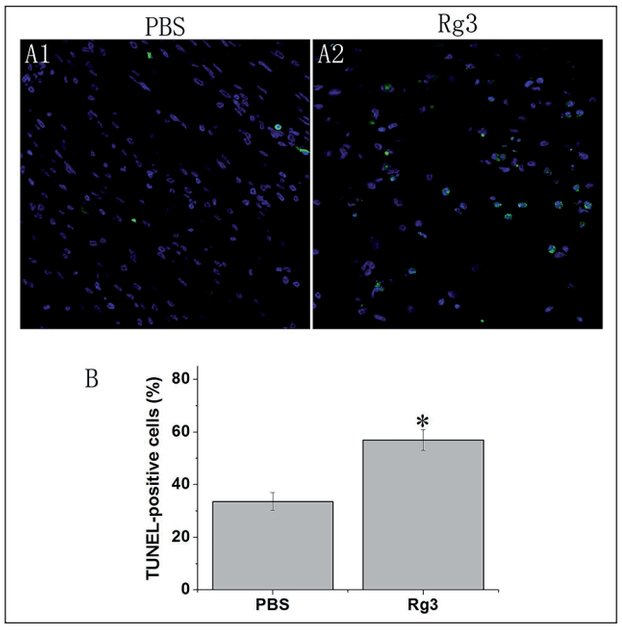

Fig. 2: TUNEL staining for apoptotic cells. More TUNEL-positive cells (with green nuclei) were evident upon Rg3 treatment (A1) compared with PBS treatment (A2), with a significant difference between groups (B; *$P < 0.05$, $n = 18$). Scale bar, 20 μm.

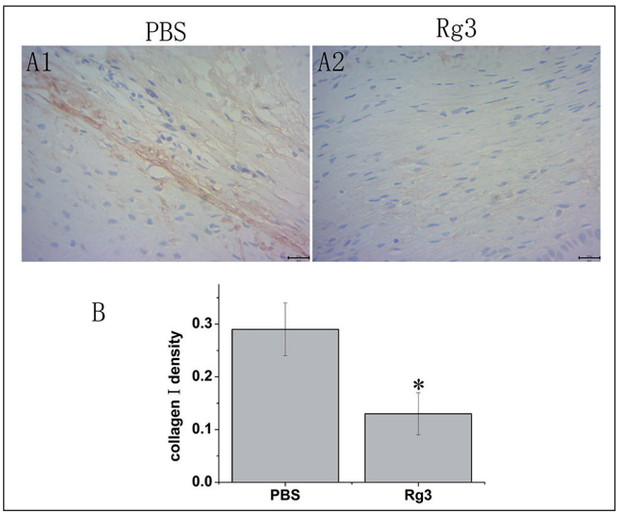

Fig. 3: Immunohistochemical staining for collagen I. (A1 and A2) Immunohistochemical (IHC)-mediated assessment of collagen I deposition in histological sections. (B) The relative collagen density. The Rg3-treated group presented markedly lower levels of collagen I compared with PBS controls (*$P < 0.05$, $n = 18$). Scale bar, 20 μm.

2.4. Impact of Rg3 on inflammation

To assess the mode of action of Rg3, we examined the effects of Rg3 on three inflammatory cytokines (IL-1β, IL-6, and TNF-α) in HS using ELISA. The levels of all three cytokines were significantly declined in the Rg3-treated group compared relative to PBS controls ($P < 0.05$). In addition, MPO levels were assessed to gauge neutrophil infiltration. As anticipated, the Rg3-treated group exhibited lower MPO levels compared with PBS controls ($P < 0.05$). Collectively, these findings suggested that Rg3 could exert anti-inflammatory effects on the HS formation (Fig. 5).

2.5. Impact of Rg3 on the NF-κB/IκB signaling

To elucidate the potential anti-inflammatory mechanisms of Rg3, we examined the NF-κB signaling pathway using western blotting and EMSA. The protein levels of NF-κB were notably decreased

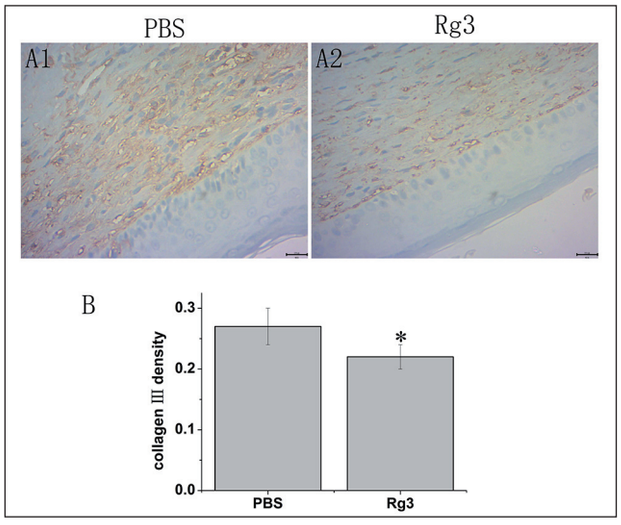

Fig. 4: Immunohistochemical staining for collagen III. (A1 and A2) IHC-mediated assessment of collagen III deposition in histological sections. (B) The relative collagen density. The Rg3-treated group presented markedly lower levels of collagen III vs. PBS controls (*$P < 0.05$, $n = 18$). Scale bar, 20 μm.

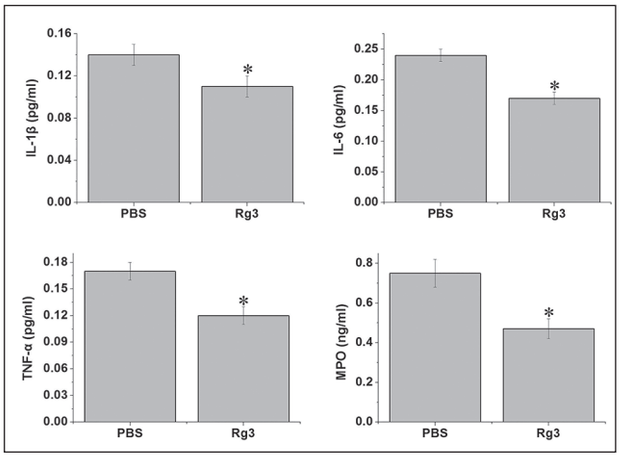

Fig. 5: The effect of Rg3 on inflammation was identified by ELISA. The expression of IL-1β, IL-6, TNF-α, and MPO in the Rg3-treated group was significantly decreased compared with PBS controls (*$P < 0.05$, $n = 18$).

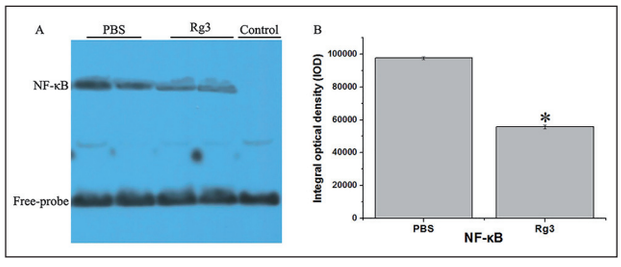

Fig. 6: (A) EMSA was performed to measure the NF-κB activity. (B) NF-κB protein levels in the Rg3-treated group were notably attenuated compared with PBS controls (*$P < 0.05$).

by Rg3, while the levels of phosphorylation of IκB (p-IκB) significantly deregulated in the Rg3-treated group relative to PBS controls ($P < 0.05$; Fig. 6 and 7).

3. Discussion

In this study, scar elevation index (SEI) measurements and histological characteristics revealed that Rg3 could suppress the HS formation. In addition, our findings established that Rg3 could inhibit the HS formation by decreasing collagen I and collagen III

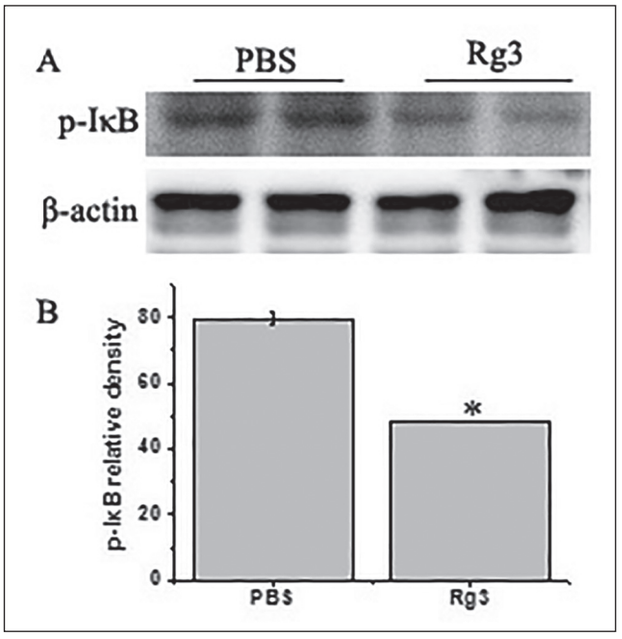

Fig. 7: (A) Levels of p-IκB were evaluated by western blotting. (B) p-IκB Levels in the Rg3-treated group were significantly deregulated compared with PBS controls (*$P < 0.05$).

synthesis, as well as by inducing fibroblast apoptosis. Our findings corroborated previous studies (Cheng et al. 2014). This study demonstrated that Rg3 treatment markedly inhibited inflammatory IL-1β, IL-6, and TNF-α production, which could reduce inflammatory neutrophil infiltration. Notably, our results suggested that Rg3 inhibited the activation of NF-κB and p-IκB activity, indicating that the anti-inflammatory effects of Rg3 in HS could be mediated by suppressing the NF-κB/IκB signaling pathway.

Inflammation closely correlates with skin wound healing. Reportedly, fetal skin wounds heal without scarring, and in mammalian embryos wounds similarly heal without the formation of scar tissue, unlike in adults. Inflammatory cell infiltration is also markedly lower in embryonic wounds, with reduced inflammatory cytokine production and a more limited duration of inflammatory wound infiltration. Wounds that occur in the oral mucosa also exhibit significantly reduced scar formation relative to cutaneous wounds, with similarly reduced levels of inflammatory cytokine production and inflammatory infiltration (Qian et al. 2016; Sorg et al. 2017). Thus, exaggerated inflammation tends to promote HS formation, which is characterized by extensive inflammatory cell infiltration and inflammatory cytokines secretion (Qian et al. 2016). However, early anti-inflammatory treatment at a wound site could effectively prevent HS formation (Cheng et al. 2014; Shan et al. 2017). Neutrophils, the first inflammatory cells recruited into a wound site, play a key role in HS pathology. Neutrophils are the first inflammatory cell type to infiltrate wounds, wherein they can mediate the removal of both pathogenic microorganisms and damaged cells. These neutrophils are able to both directly phagocytose target cells, and to mediate killing through their release of cytolytic granules as well as neutrophil extracellular traps. This neutrophil-mediated inflammatory activity is under strict spatial and temporal regulation. When unregulated, these cells can secrete a range of inflammatory cytokines, stimulating fibroblast proliferation and excessive collagen accumulation, thereby leading to the HS formation. Conversely, it was reported that the depletion of neutrophils accelerates wound closure in mice (Qian et al. 2016; Sorg et al. 2017). Moreover, previous studies demonstrated that decreased neutrophils infiltration correlates with the inhibition of the HS formation (Liu et al. 2014; Wang et al. 2015; Shan et al. 2017). This study clearly demonstrated that Rg3 treatment markedly ameliorated neutrophils infiltration into the HS site. Several inflammatory factors IL-1β, IL-6, and TNF-α are involved during

HS to form an inflammatory cascade event. The elevated release of proinflammatory cytokines produced by inflammatory cells have been noted in HS. Meanwhile, the proinflammatory cytokines can attract inflammatory cells to the wound, thereby amplifying the inflammatory response. Reportedly, therapeutic interventions that attenuate inflammatory cytokines could be effective in the treatment of HS (Shaw et al. 2010). This study demonstrated that Rg3 treatment markedly inhibited IL-1β, IL-6, and TNF-α production, consistent with the effects of Rg3 in the context of certain other inflammatory diseases (Cheng and Li 2016; Lee et al. 2016).

Overall, our findings demonstrated that Rg3 exerted anti-inflammatory effects on the HS formation by inhibiting the inflammatory cytokine production (IL-1β, IL-6, and TNF-α) and reducing inflammatory neutrophil infiltration.

The NF-κB/IκB signaling pathway is well-known to be a central regulator of inflammation. Although the NF-κB/IκB signaling is involved in the process of HS formation (Ishise et al. 2015; Chen et al. 2017; Gong et al. 2017), the specific underlying mechanisms of inflammation remain unclear. In addition, it remains unclear as to whether Rg3 could modulate the NF-κB/IκB signaling pathway in the context of the HS formation. The transcription factor NF-κB is typically sequestered in a complex with IκB in the cytoplasm, but when phosphorylated IκB is degraded allowing for the subsequent translocation of NF-κB into the nucleus. This leads to the expression of target genes such as IL-1β, IL-6, and TNF-α (Rothschild et al. 2018; Staal and Beyaert 2018). In this study, IκB degradation occurred once it was phosphorylated, leading NF-κB nuclear translocation and upregulation of genes associated with HS. We further found that Rg3 was able to inhibit IκB phosphorylation, thus reducing NF-κB-mediated inflammation in the context of HS. Overall, this study demonstrated that Rg3 could markedly suppress the NF-κB/IκB signaling pathway, thereby ameliorating neutrophil infiltration and inhibiting inflammatory cytokine production, leading to suppressing the HS formation. However, this study has some limitations, which need further investigation and future improvements. Additional controlled trials and a comprehensive examination of the inflammation downstream of the NF-κB/IκB signaling pathway would enable better evaluation of the therapeutic value of Rg3 in the future.

In conclusion, this study suggests that the anti-scarring properties of Rg3 might result from inhibiting inflammation by modulating the NF-κB/IκB signaling. Perhaps, this study might support the use of Rg3 as a means of treating or preventing the HS formation.

4. Experimental

4.1. Animals

All study protocols were approved by the Ethics Committee of Anhui University of Traditional Chinese Medicine (Hefei, China). We obtained Newland white rabbits of either sex (weighing 2.5–3.0 kg) from the Laboratory Animal Center of Anhui University of Traditional Chinese Medicine; all animals were individually housed in a standard environment with free food/water access.

4.2. Rabbit HS model and treatment

We constructed a rabbit ear HS model using a previously reported method (Morris et al. 1997). Briefly, rabbits were anesthetized using pentobarbital sodium (3%, intraperitoneal injection) and operated under aseptic conditions. Overall, six full-thickness wounds extending into the cartilage were created by a 6-mm punch biopsy of the ventral surface of both ears, removing the epidermal, dermal, and perichondrial layers. Then, manual pressure was used to achieve hemostasis, and any necrotic or infected wounds were excluded for downstream analyses.

The model rabbits were separated at random into two groups–PBS-treated group and Rg3-treated group–each containing 18 scars. For treatment, the Rg3 concentration was set at 4 mg/L, as described previously (Cheng et al. 2014). Rg3 was injected into the edge and center of the wound immediately after operation and every 3 days thereafter until day 14, whereas PBS controls received an equal volume of PBS. On postoperative day 28, animals were sacrificed and wounds were collected.

4.3. Histological analysis and immunohistochemistry

The scars were bisected at the highest point and then fixed with formaldehyde (4%). Then, sections underwent standard dehydration, paraffin embedding, sectioning at 5-μm thickness, and H&E staining. Next, samples were assessed using an Eclipse 80i light microscope and subsequent analysis were performed via light microscopy (Nikon, Tokyo, Japan). Using the scar elevation index (SEI), which calculates the ratio of the total scar area to the normal tissue area underneath a scar, we evaluated the degree of dermal hypertrophy, as described previously (Morris et al. 1997). An SEI of 1 indicates wound healing in the absence of hypertrophy, while an index > 1 defines HS formation.

Once samples were deparaffinized and rehydrated, H_2O_2 (3%) was used to quench endogenous peroxidase activity, and normal goat serum was used to block any nonspecific binding. Next, sections were probed using primary rabbit antibodies against collagen I (1:20; Abcam) and collagen III (1:20; Biorbyt, UK) overnight at 4 °C. Sequentially, the second antibody (Abcam) was then used, followed by incubation with horseradish peroxidase–streptavidin. Eventually, we performed color development with diaminobenzidine and hematoxylin counterstaining. Meanwhile, routine negative controls also were conducted, and slides were observed using an optical microscope.

4.4. TUNEL staining

To detect the HS cell apoptosis, we used the TUNEL staining approach based on the directions provided with the In Situ Cell Death Detection Kit (Fluorescein, Switzerland). The apoptotic cells (TUNEL-positive), which exhibited green nuclei, were counted in each section using an optical microscope.

4.5. ELISA

We measured the concentrations of MPO, IL-1β, IL-6, and TNF-α in HS tissues using an appropriate ELISA kit (USCN, Wuhan, China) per provided directions, measuring OD at 450 nm on a plate microreader (NanoDrop Spectrophotometer, Thermo Fisher Scientific Inc., Wilmington).

4.6. Western blotting

We conducted western blotting as following. Briefly, total protein was extracted from the HS tissues using RIPA lysis buffer. Protein concentrations were evaluated using the bicinchoninic acid (BCA) method. Then, we separated equivalent amounts of protein by 10% SDS–PAGE, which were transferred onto PVDF membranes; these membranes underwent blocking using 5% non-fat milk and were, then, probed with anti-p-IκB (1:500; Biorbyt) overnight at 4 °C. Subsequently, the membranes were incubated for 1.5 h with secondary HRP-conjugated anti-rabbit IgG at room temperature. Next, proteins were visualized using enhanced chemiluminescence (ECL) and analyzed using a digital imaging system. Finally, the band intensity was normalized to β-actin, which was served as an equal protein loading control.

4.7. EMSA

The HS tissues were cut into pieces and homogenized. Then, the homogenate was immediately incubated for 5 min on ice prior to centrifugation. Cytoplasmic extracts were then isolated from prior to storage at -80 °C, while the remaining nuclei were resuspended for 20 min on ice. Nuclear lysates were then spun down for 10 min at 12,000 rpm, and supernatants were frozen at -80 °C. Then, protein concentrations were evaluated using the BCA kit (Beyotime, China), following which EMSA was performed. A total of 5 μg of nuclear extracts were combined with a double-stranded NF-κB oligonucleotide probe (forward: 5′-AGTTGAGGGGACTTTCCCAGGC-3′; reverse: 5′-GCCTGGGAAAGTCCCCTCAACT-3′) at room temperature for 30 min per the manufacturer's instructions (Chemiluminescent EMSA Kit, GS009, Beyotime). Subsequently, the DNA–protein complexes were separated by electrophoresis in 6% polyacrylamide gels and were transferred to a nylon membrane. Finally, the gels were dried, exposed to film, and analyzed using the Image-pro software.

4.8. Statistical analysis

In this study, we used SPSS v20.0 for all statistical analyses. Data are means±SD. Furthermore, Student's *t*-tests were used to compare between-group differences, with a significance threshold of $P < 0.05$.

Acknowledgements: The research was supported by the Natural Science Research Foundation of Colleges and Universities in Anhui Province (grant number: KJ2017A286).

Conflicts of Interests: The authors declare no conflict of interest.

References

Chen YY, Lu YH, Ma CH, Tao WW, Zhu JJ, Zhang X (2017) A novel elastic liposome for skin delivery of papain and its application on hypertrophic scar. Biomed Pharmacother 87: 82-91.

Cheng L, Sun X, Hu C, Jin R, Sun B, Shi Y, Cui W, Zhang Y (2014) In vivo early intervention and the therapeutic effects of 20(S)-ginsenoside Rg3 on hypertrophic scar formation. PLoS One 9: e113640.

Cheng Z, Li L (2016) Ginsenoside Rg3 ameliorates lipopolysaccharide-induced acute lung injury in mice through inactivating the nuclear factor-κB (NF-κB) signaling pathway. Int Immunopharmacol 34: 53-59.

Gong YF, Zhang XM, Yu J, Huang TY, Wang ZZ, Liu F, Huang XY (2017) Effect of recombinant human endostatin on hypertrophic scar fibroblast apoptosis in a rabbit ear model. Biomed Pharmacother 91: 680-686.

Ishise H, Larson B, Hirata Y, Fujiwara T, Nishimoto S, Kubo T, Matsuda K, Kanazawa S, Sotsuka Y, Fujita K, Kakibuchi M, Kawai K (2015) Hypertrophic scar contracture is mediated by the TRPC3 mechanical force transducer via NFkB activation. Sci Rep 5: 11620.

Lee H, Jang Y (2018) Recent understandings of biology, prophylaxis and treatment strategies for hypertrophic scars and keloids. Int J Mol Sci 19: e711.
Lee IS, Uh I, Kim KS, Kim KH, Park J, Kim Y, Jung JH, Jung HJ, Jang HJ (2016) Anti-inflammatory effects of ginsenoside Rg3 via NF-κB pathway in A549 cells and human asthmatic lung tissue. J Immunol Res 2016: 7521601.
Liu S, Jiang L, Li H, Shi H, Luo H, Zhang Y, Yu C, Jin Y (2014) Mesenchymal stem cells prevent hypertrophic scar formation via inflammatory regulation when undergoing apoptosis. J Invest Dermatol 134: 2648-2657.
Morris DE, Wu L, Zhao LL, Bolton L, Roth SI, Ladin DA, Mustoe TA (1997) Acute and chronic animal models for excessive dermal scarring: quantitative studies. Plast Reconstr Surg 100: 674-681.
Qian LW, Fourcaudot AB, Yamane K, You T, Chan RK, Leung KP (2016) Exacerbated and prolonged inflammation impairs wound healing and increases scarring. Wound Repair Regen 24: 26-34.
Rothschild DE, McDaniel DK, Ringel-Scaia VM, Allen IC (2018) Modulating inflammation through the negative regulation of NF-κB signaling. J Leukoc Biol 103: 1131-1150.
Shan S, Zhang Y, Wu M, Yi B, Wang J, Li Q (2017) Naringenin attenuates fibroblast activation and inflammatory response in a mechanical stretch-induced hypertrophic scar mouse model. Mol Med Rep 16: 4643-4649.
Shaw TJ, Kishi K, Mori R (2010) Wound-associated skin fibrosis: mechanisms and treatments based on modulating the inflammatory response. Endocr Metab Immune Disord Drug Targets 10: 320-330.
Sorg H, Tilkorn DJ, Hager S, Hauser J, Mirastschijski U (2017) Skin wound healing: an update on the current knowledge and concepts. Eur Surg Res 58: 81-94.
Staal J, Beyaert R (2018) Inflammation and NF-κB signaling in prostate cancer: Mechanisms and clinical implications. Cells 7: e122.
Wang H, Chen Z, Li XJ, Ma L, Tang YL (2015) Anti-inflammatory cytokine TSG-6 inhibits hypertrophic scar formation in a rabbit ear model. Eur J Pharmacol 751: 42-49.
Wang L, Li X, Song YM, Wang B, Zhang FR, Yang R, Wang HQ, Zhang GJ (2015) Ginsenoside Rg3 sensitizes human non-small cell lung cancer cells to γ-radiation by targeting the nuclear factor-κB pathway. Mol Med Rep 12: 609-614.